EasyChair Preprint

№ 7784

Analysis of the Flow and Transmission Performance of Magnetorheological Brakes Based on Shear-Squeeze Mode

Hang Gong, Ruizhi Shu, Guanghui Hu, Wenjian Chen, Yang Xiong and Jin Huang

April 12, 2022

2022CFPMCE+Journal of Vibroengineering

+Journal of Dynamics, Monitoring and Diagnostics

Analysis of the flow and transmission performance of magnetorheological brakes based on shear-squeeze mode

Hang Gong[1], Ruizhi Shu[2], Guanghui Hu[3], Wenjian Chen[4], Yang Xiong[5], Jin Huang[6]
College of Mechanical Engineering, Chongqing University of Technology, Chongqing, China
[6]Corresponding author

E-mail: [1]*gonghang2021@qq.com*, [2]*ruizhishu@cqut.edu.cn*, [3]*huguanghui@stu.cqut.edu.cn*, [4]*chenwenjian@2020.cqut.edu.cn*, [5]*xiongyang2019@qq.com*, [6]*jhuangcq@cqut.edu.cn*

Abstract. Aiming at the complex structure of the existing squeezed magnetorheological brakes, a disc-type magnetorheological brake strengthened by self-squeezing using wedge-shaped gaps is proposed in this article. Four rectangular slots were evenly distributed on the rotor surface of this actuator, and the pressure generated by the gap variation squeezes the magnetorheological fluid, which makes the actuator more compact while improving its working performance. The magnetic field was analyzed based on the finite element method, the magnetic and mechanical properties of the magnetorheological fluid under different currents were obtained. Then, on the basis of computational fluid dynamics, the flow field analysis of the magnetorheological fluid was carried out, and the cloud diagram of squeezing stress distribution along the circumference was obtained. At last, the flow equation of magnetorheological fluid is derived based on the Navier-Stokes equation and the squeeze strengthening model, and the relationship between the torque, current, and squeeze stress was established. The results show that the wedge gap causes the periodic change of fluid squeeze stress, and the shear yield stress of magnetorheological fluid increases significantly after squeeze strengthening. When the input current is 2.0 A, the shear yield stress is 67.7 kPa and the torque is 24.8 N·m, which is about 46.2 % higher compared with the un-squeezed state.

Keywords: magnetorheological fluid brake; wedge gap squeeze; flow; torque; squeeze-strengthening effect

1.Introduction

Magnetorheological fluid(MRF) is a new magnetic smart material, MRF is a suspension formed by polarizable magnetic particles in a basic fluid.[1,2].The unique magnetorheological effect of MRF is shown by the fact that MRF behaves as a Newtonian fluid when no magnetic field is applied; Under the action of magnetic field, the dispersed magnetic particles in MRF can form a chain-like structure along the magnetic field direction in a very short time, which transforms the fluid from a free-flowing state to a non-Newtonian fluid form and exhibits mechanical properties similar to those of a solid [3,4].For the magnetorheological effect with the advantages of reversible, rapid response, stepless speed regulation, MRF has a wide range of applications in the clutch, brake and other mechanical transmission fields [5,6].

Magnetorheological brakes are new brakes that use MRF as the power medium to obtain controlled braking torque, but the small rotating torque of magnetorheological brakes seriously affects the development of magnetorheological brakes. Domestic and foreign scholars have conducted a lot of research on MRF and magnetorheological devices, and have proposed various solutions to increase the braking torque. Sun et al[7] have Chosen 10 different MRF material samples for experiments and analysis, test the mechanical properties and material parameters of MRF material samples, study the influence of different factors such as magnetic induction strength and temperature on the performance of magnetorheological actuator, and prove the reliability and practicality of

magnetorheological actuator; Yang et al[8] had established a mechanical and structural model of MRF under microscopic, combined with theoretical analysis of the characteristics of the two modes of operation of shear and extrusion; Wu et al[9] had proposed a new multi-disc magnetorheological drive for high-power applications, designed and optimized the structure of the device, and measured through analysis and experiments that the magnetorheological drive can generate a maximum torque of 1800N-m; Mazlan et al[10] through experiments to verify the physical properties of MRF in extrusion mode, the results show that the physical properties of MRF after extrusion are greatly improved; Xiong et al[11] had proposed a combined MRF and electrothermal shape memory alloy transmission device, using shape memory alloy to improve the torque of the magnetorheological device, the torque magnitude of the device was calculated by simulation analysis and verified experimentally. The above research mainly focuses on improving the magnetorheological device torque by changing the frictional characteristics and magnetic properties of MRF, and there is less research on improving the transmission torque by relying on the rheological properties of MRF itself. Because the MRF has special fluid properties, by changing the flow rate and pressure of the MRF in the working gap will also have a certain effect on the magnetorheological device[12,13], Therefore some scholars have used Computational fluid dynamics(CFD) techniques to study the flow properties of MRF,DA et al[14] through CFD and Finite element method (FEM) finite element method, a comprehensive simulation study of magnetorheological fluid journal bearings was conducted, and the journal bearing characteristics such as eccentricity, attitude angle, oil flow and friction coefficient were calculated, and the functions of magnetic field and L/D bearing ratio were listed; Susan-Resiga et al[15] had discussed the setting of CFD model of magnetorheological fluid and its influence on the results. Proposes two magnetorheological valves based on parallel plate simplification, and concludes that the pressure loss of magnetorheological fluid at the inlet and outlet has less influence on the pressure drop in the gap than that of conventional hydraulic fluid.

In this paper, based on the rheological characteristics of MRF, a magnetorheological brake based on shear-extrusion mode is designed and proposed. The working principle of the brake is analyzed, the magnetic field model and the flow field model of MRF in the brake are established, the magnetic field and the flow field of the brake are studied by using FEM and CFD techniques respectively, and the magnetic field distribution state and the flow field distribution state in the brake are obtained, and the braking torque versus current curve of the brake is derived on the basis of the Navier-Stokes equation and the extrusion strengthening model.

2. Working principle

The MRF brake structure schematic diagram is shown in Figure 1. The brake is mainly composed of the following parts: 1 - coil, 2 - housing, 3 - bearing, 4 - active shaft, 5 - rotor, 6 - mounting base, 7 - MRF, etc., where the mounting base is fixedly connected to the frame by bolts and the coil is fixedly sealed inside the housing by PVC. The working principle of this brake is as follows.

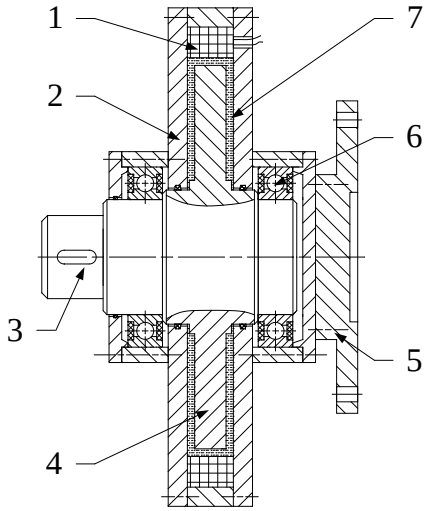

Figure 1. MRF brake schematic diagram

(1) In the initial state, the MRF is in the state of Newtonian fluid without the influence of magnetic field when the coil has not been energized, and the input shaft relies on the braking torque generated by the viscosity of MRF under zero magnetic field, which cannot produce a significant braking effect.

(2) In the braking process, the coil is energized to generate a magnetic field, the magnetic particles in the MRF are arranged into chains under the influence of the magnetic field, and the MRF is transformed from a Newtonian fluid to a viscoplastic solid, and its shear yield stress is strengthened, relying on the shear yield stress MR brake can produce an obvious braking effect. At the same time, due to the rotor wall processing four rectangular grooves, rectangular groove area and the disc area to form a wedge gap, when the MRF from the rectangular groove area will generate squeezing pressure, under the action of pressure MRF will produce squeeze-strengthening effect, and MRF shear yield stress is increased, the braking performance is increased.

(3) End of braking, the coil power, and the MRF is returned to a Newtonian fluid by the viscoplastic body after the magnetic field disappears, the MR brake ends braking.

3. Design and finite element analysis

3.1 Analysis of the magnetic fields

In order to increase the braking torque generated by the MRF brake, the magnetic lines of force in the magnetic field should cross the MRF as perpendicular as possible and maximize the MRF operating gap to a high intensity magnetic field. In ordered to analyze the magnetic field of the brake unit as a whole under the operating condition, the magnetic flux distribution is simulated by the finite unit method, and the simplified model of magnetic field analysis is shown in Figure 2.

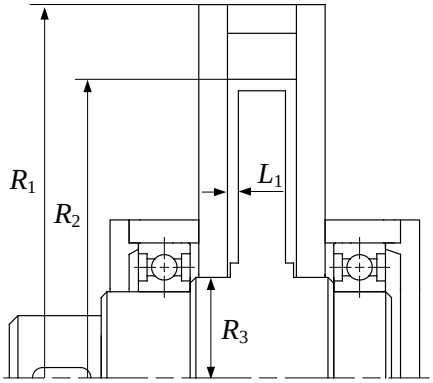

Figure 2. 2D axisymmetric simplified model

The structure parameters of this brake are shown in Table 1.

Table 1. Structure parameters of the MR transmission device (mm)

R_1	R_2	R_3	L_1
50	37	20	1.5

The 2D axisymmetric FEM model is established by the magnetic circuit diagram shown in Figure 2, and the calculated results of the magnetic circuit analysis are used as the magnetic field excitation conditions of the magnetic finite element analysis (FEA). To improve the accuracy of the magnetic FEA, the nonlinear permeability of the material is considered, in which the input shaft, output shaft and rotor, etc., are all made of 20# steel, the MRF-J01T is provided by Chongqing Institute of Materials Research, and the MRF material parameters are shown in Table 2[16].

Table 2. Material parameters of the MRF (MRF-J01T)

φ	μ_0	μ_f
25%	400	$4\pi \times 10^{-7}$H/m
μ_p	σ_s^2/τ_0^2	δ
10	9	1.202

In Table 2. φ is the MRF volume fraction; μ_0 is the relative permeability of the base fluid; μ_f is the vacuum permeability; σ_s is the MRF shear yield stress; τ_0 is the initial shear stress; δ is the material coefficient; μ_p is the relative magnetic permeability of the magnetic particles.

The magnetization curves of 20# steel and MRF are shown in Figure 3 and Figure 4, respectively.

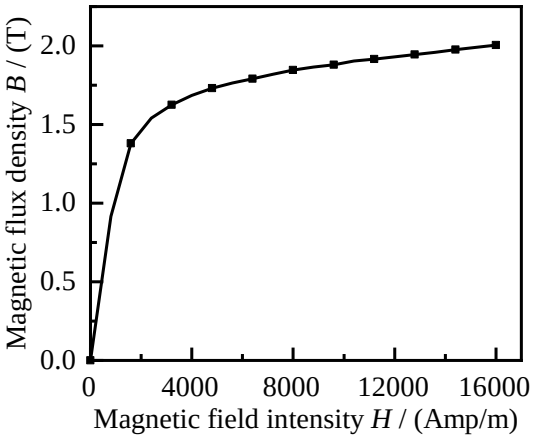

Figure 3. 20# steel magnetization curve

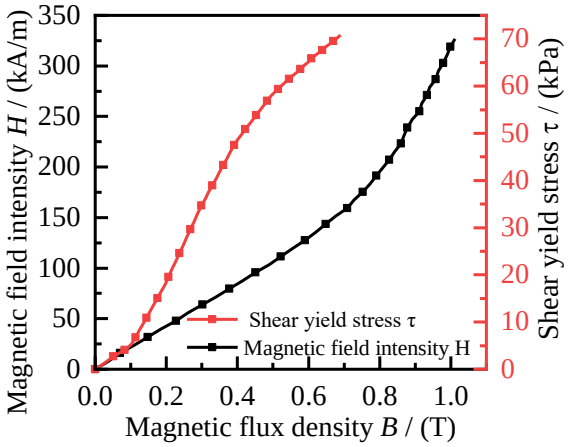

Figure 4. MRF-J01T magnetization curve

The relationship between the magnetic flux density B and the shear yield stress $\tau(B)$ is obtained from the Figure 4, and the fitted equation is as follows

$$\tau(B) = 76 \sin\left(\frac{188B - 1}{100}\right) \tag{1}$$

The magnetic field analysis is set to steady-state magnetic FEA, the boundary condition is set to Balloon, and the relative permeability is 1. The number of turns of the coil is set to 100, and the 3D magnetic flux density and magnetic line distribution clouds are shown in Figure 5 while the currents are set to 0.5 A, 1.0 A, 1.5 A, and 2.0 A, respectively. The magnetic lines are perpendicular to the MRF working gap so that the maximum shear yield stress can be generated after MRF chainization.

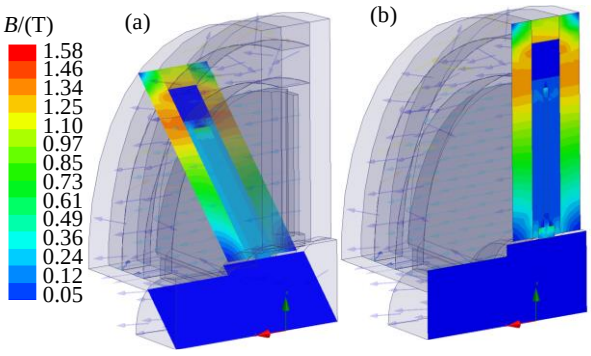

(a) disc area (b) rectangle groove area

Figure 5. Cloud diagram of 3D magnetic flux density (I=2.0A)

The magnetic flux density of the corresponding cross-sections in different regions are intercepted in Figure 5. In Figure 5(a), the maximum and the minimum values of magnetic flux density in the disc surface region are 0.31 T and 0.14, respectively, with the average magnetic flux density of 0.22 T. As a comparison, the maximum, minimum and average values of the magnetic flux density at the MRF working gap in the rectangular slot region (Figure 5(b)) are 0.35 T, 0.32 T, and 0.33 T, respectively. It shows that the shape of the rotor surface will affect the flux distribution and thus the working performance of MRF under the no-flow state. Combining Equation (1) and Figure 5, we can get the radial magnetic flux density and shear yield stress of MRF under different currents, as shown in Figure 6.

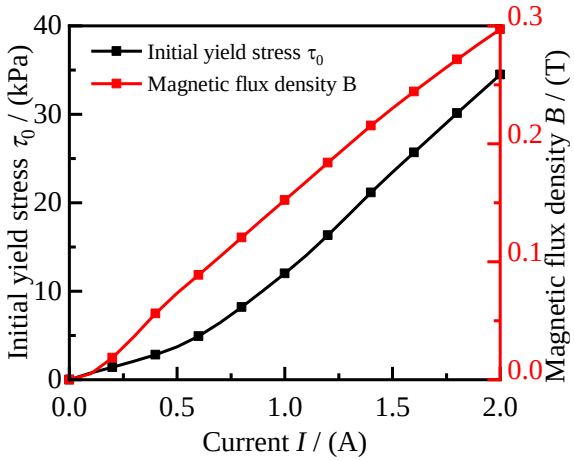

Figure 6. Radial magnetic flux density and shear yield stress of MRF under different currents

From Figure 6, it can be observed that the magnetic flux density of the MRF increases as the coil current increases. When the current increases from 0 to 2.0 A, the magnetic flux density rises from 0 T to 0.3 T accordingly. The initial yield stress under the magnetic field is approximately linearly related to the current. And the maximum value of the initial yield stress generated by MRF is 34.5 kPa when the current is 2.0 A.

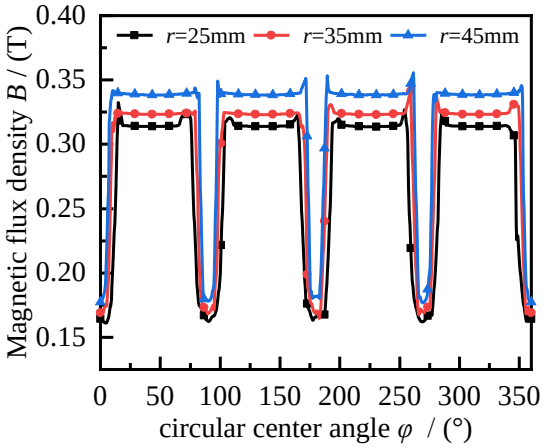

Figure7. Relationship between magnetic flux density and circular center angle

Figure 7 shows the changing law of circumferential magnetic flux density on the shear surface of the MRF working gap. As shown when the coil current is 2.0 A, the relationship between magnetic flux density and circular center angle into a periodic change. The fluctuation range of magnetic flux density in the figure is large, and the region of maximum value corresponds to the four rectangular slot regions on the rotor, in which the magnetic flux density and the effective working radius are approximately linear. When the effective working radius of MRF increases from 25 mm to 45 mm, the average magnetic flux density increases from 0.28 T to 0.35 T.

3.2 Analysis of the flow field

In order to analyze and describe the flow properties and pressure distribution of the brake more accurately, a

flow field analysis of the brake was performed based on the CFD method. The following assumptions are made now: (1) the MRF is an incompressible fluid; (2) there is no relative slip motion between the housing surface and the MRF; (3) the MRF is all in a non-Newtonian fluid state under the action of the magnetic field; (4) the effect of the shear strain rate on the viscosity is neglected; (5) the MRF does not reach magnetic saturation under any current and the magnetic field is uniformly distributed; (6) the inertia force of the MRF is neglected. The simplified model of flow field analysis is shown in Figure 8.

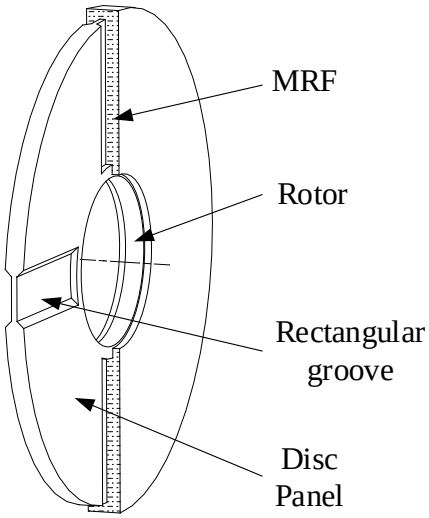

Figure 8. Simplified model of the rotor

In the CFD numerical analysis, all structural parameters are consistent with the magnetic FEA, and in the analysis process, the rotor speed ω = 63 rad/s. The MRF flow model is selected as laminar flow because the MRF has assumed non-Newtonian fluid all over the working gap; with the fluid properties set to the Bingham model and the zero-field viscosity η0=0.38 Pa·s in the Bingham model. The remaining parameters are shown in Table 3 below, and the solution calculation is started after all settings are completed. The computational solution requires the residuals of all variables to be at least less than 1/10000 before the results are considered valid for convergence

Table 3. Parameters of the Bingham model

Current I/(A)	Magnetic flux density B/(T)	Initial shear yield stress τ_0/(kPa)
0.50	0.07	3.71
1.00	0.15	11.95
1.50	0.23	23.46
2.00	0.32	34.47

From the CFD analysis, the flow velocity and circumferential direction distribution of the MRF in the Bingham model with magnetic flux density of 0.32 T and initial yield stress of 34.47 kPa are shown in Figure 9.

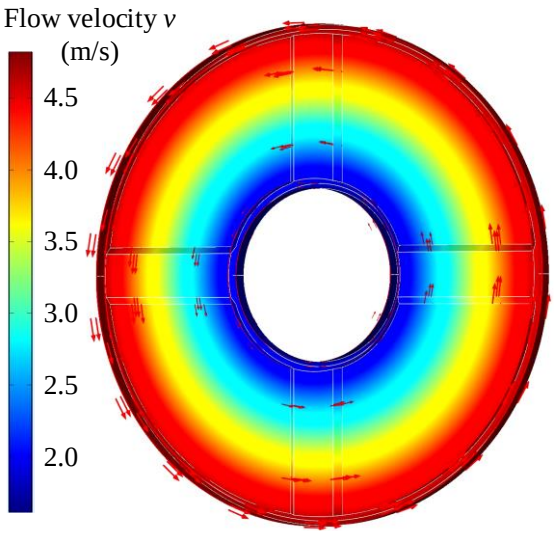

Figure 9. Flow velocity and circumferential direction distribution of the MRF (I=2.0A)

As presented in Figure 9, the flow velocity near the rotor edge is up to the maximum value of 4.5 m/s, and the minimum value is 2.0 m/s near the rotation center. The MRF flow velocity increases continuously with the increase of the rectangular slot radius, and the MRF flow direction is clockwise in line with the rotor rotation.

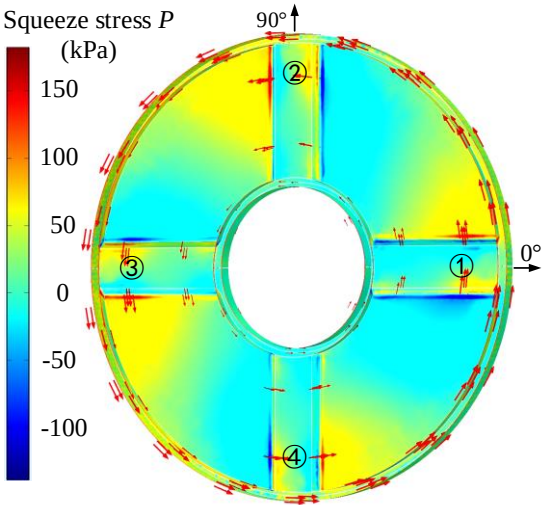

Figure 10. Cloud diagram of the pressure distribution (I=2.0A)

MRF flows into the disc gap from the rectangular groove gap during the flow of MRF in the gap. The convergence gap formed by the rectangular slot and the disc allows the MRF to generate squeeze stresses. As shown in Figure 10, MRF under the action of rotor rotation, the extreme value of squeeze stress appears on both sides of the rectangular groove. From the flow direction, it can be seen that the positive pressure is distributed on the MRF outflow side of the rectangular groove. Since the rectangular grooves in the rotor wall are distributed in a periodic pattern, the squeeze stress distribution cloud appears in four periodic distribution relationships. The absolute values of the squeeze stresses on the outflow side and inflow side reach the maximum in the rectangular groove ① area. The squeezing pressure generated by the wedge gap causes a strong squeezing-strengthening effect on the local MRF in the working gap, thus achieving an improvement in the braking performance of the MRF brake.

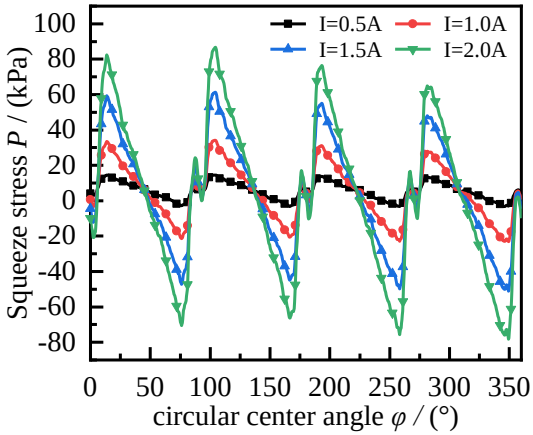

Figure11. Relationship between squeeze stress and circular center angle

MRF is subjected to cyclically varying squeeze stress on the rotor surface at different currents. As shown in Figure 11, The initial value of the squeeze stress is different because of the different currents, For example, in the first cycle, At different currents, the absolute value of the extrusion stress reaches a maximum at positions 25° and 75°, respectively15kPa,34kPa,61kPa,80kPa. It means that the squeeze stress on MRF increases with the increase of current. At the same current, when the current is 2.0A, the initial absolute value of squeeze stress is 10kPa. As the circular center angle increases, the absolute value of squeeze stress reaches a maximum of 80kPa at 25°. Indicating that when MRF flows from the rectangular groove area to the disc area subjected to a substantial increase in the squeeze stress. The wedge-shaped gap formed by the two is able to produce an squeeze effect on MRF.

4. Analysis of the braking torque

4.1 Naiver-Stokes

The Bingham constitutive model can describe the rheological properties of MRF in the presence of a magnetic field, and the constitutive relationship can be expressed as[17].

$$\tau = \tau(B)\mathrm{sgn}(\dot{\gamma}) + \eta\dot{\gamma} \tag{2}$$

where τ is the shear yield stress of MRF after extrusion, $\tau(B)$ is the function of MRF shear yield stress and magnetic induction strength, $\mathrm{sgn}(\dot{\gamma})$ is the sign function, η is the MRF viscosity coefficient, and $\dot{\gamma}$ is the MRF shear strain rate.

When the inner diameter of the MRF brake is r_3, the outer diameter is r_1, the rotational speed difference is ω, and the MRF thickness is L_1, the shear strain rate of MRF can be expressed as[18]

$$\dot{\gamma} = \frac{\mathrm{d}\omega}{\mathrm{d}L_1} r \tag{3}$$

where ω is the rotational speed and r is the MRF working radius.

The braking torque of the MRF brake before squeezing can be expressed as [19]

$$M_{\mathrm{MRF}} = \frac{2\pi}{3}(R_1^3 - R_3^3)\tau(B) + \frac{\pi\eta}{2L_1}(R_1^4 - R_3^4)\omega \tag{4}$$

From equation (4) it can be seen that the disc MRF brake braking torque consists of two parts: shear braking torque and viscous braking torque. The first part of the equation is the braking moment generated by the shear yield stress, which is obtained from the rheological properties of the MRF, and its magnitude is related to the magnetic field, while the second term is the zero-field viscous braking torque, which is related to the zero-field viscosity of the MRF, the rotor speed and the geometry of the rotor, with no applied magnetic field. However, equation (4) ignores the influence of rotor shape on the operating characteristics of MRF and cannot accurately solve for the braking torque generated by MRF after extrusion strengthening. To accurately analyze the enhancement of MRF working performance after squeeze strengthening, the following derivation of MRF pressure and flow rate of the disc brake flow model is shown in Figure 12.

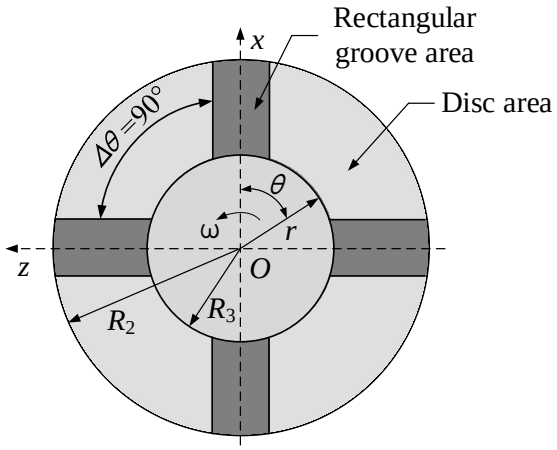

Figure 12. Schematic diagram of MRF flow model

According to the MRF flow model, combined with the proposed assumptions, the edge effect of the inner and outer radius is neglected due to the MRF working gap thickness $L_1 \ll (R_2 - R_3)$. Also, it is assumed that gravity is negligible and the centrifugal force due to centrifugal acceleration is negligible compared to the force due to viscous stress gradient and pressure gradient because the rotor speed is low enough. Therefore, the inertia term in the Navier-Stokes equation can be neglected, and the Navier-Stokes equation ignoring the inertia term in the semi-cylindrical coordinate system is [20]

$$\frac{1}{r}\frac{\partial p}{\partial \theta} = \eta\left[\frac{\partial}{\partial r}\left(\frac{1}{r}\frac{\partial}{\partial r}(rv_\theta)\right) + \frac{\partial^2 v_\theta}{\partial z^2} + \frac{2}{r^2}\frac{\partial v_r}{\partial \theta}\right] \tag{5}$$

Where $\partial p/\partial\theta$ is the pressure gradient along the rotation direction, v_θ and v_r are the velocity in the radius direction and rotation direction, respectively. The pressure gradient on the left is equal to the diffusion of the circumferential momentum on the right, and the pressure gradient varies with the viscous stress applied to the fluid by the rotor, so increasing the viscous stress will increase the pressure gradient.

In the cylindrical coordinate system, the component of the velocity at any position in the z-axis is approximately 0. In addition, the MRF working clearance is much smaller than the rotor circumference, so the Navier-Stokes equation can be reduced to the continuity equation, and the continuity equation is[21]

$$\frac{1}{r}\frac{\partial}{\partial r}(rv_\theta) = 0 \tag{6}$$

Where r and v_r are a constant, when $r = R_1$, $v_\theta = 0$. When $v_r = 0$, the pressure gradient in z direction and r direction is

$$\begin{cases}\dfrac{\partial p}{\partial z} = 0 \\ \dfrac{\partial p}{\partial r} = 0\end{cases} \tag{7}$$

Where the pressure gradient in z direction and r direction is constant.

Combined with the structural parameters of MRF brakes, the relationship between MRF working gap thickness L_1 and radius R_2 and R_3 can be expressed as

$$\frac{L_1}{R_2 - R_3} \ll 1 \tag{8}$$

Since the MRF working gap is very small, the variation of v_θ in the z-direction along L_1 is much larger than the variation of v_θ in the r-direction along R_2-R_3, when v_θ=0. The second term on the right side of equation (5) is ignored, and the simplified equation is obtained as follows[22]

$$\frac{1}{r}\frac{\partial p}{\partial \theta} = \mu\frac{\partial^2 v_\theta}{\partial z^2} \tag{9}$$

Based on the assumptions made above for the MRF flow model, the circumferential velocity v_θ does not vary with position at this time, and according to the mass conservation theorem, the relationship between MRF pressure and circular angle derived from the simplification of equation (9) can be expressed as

$$\frac{\partial p}{\partial \theta} \approx \frac{\Delta P}{\Delta \theta} \tag{10}$$

Where ΔP is the pressure stress difference between the low pressure region and the high pressure region, and $\Delta \theta$ is the angle of the circle corresponding to the arc length.

4.2 Squeeze-strengthening effect

The relationship between pressure and angle is obtained from equation (10), and the MRF under pressure will produce a squeeze-strengthening effect, at which time the shear yield stress τ_y in the MRF consists of the shear yield stress τ_m generated by the magnetic dipole action and the shear yield stress τ_f generated by the mutual friction of the magnetic particles. The experimentally modified shear yield stress τ_y is[23]

$$\tau_y = K_1\tau_m + K_2\tau_f \tag{11}$$

Where, K_1 and K_2 are correction factors, shear yield stress τ_m is

$$\tau_m = 36\varphi\mu_f\mu_0\beta^2 H_0^2 \left(\frac{r}{d}\right)^3 \delta\dot{\gamma} \tag{12}$$

where β is the material coefficient, expressed as $\beta = \frac{\mu_p-\mu_0}{\mu_p+2\mu_0}$, the parameters are shown in Table 2. The shear yield stress τ_f generated by the magnetic particles rubbing against each other is

$$\tau_f = \frac{Q\tau_0^2[\frac{\sigma_s^2}{\tau_0^2}(1-Q^2)]^{1/2}}{[\sigma_s^2(1-Q^2)]}P \tag{13}$$

where Q is the correction factor, P is the MRF subjected to squeeze stress, and the remaining parameters are shown in Table 2.

Combining equations (10) and (11), as well as the CFD analysis results, the variation of shear yield stress of MRF under the action of squeezing pressure can be obtained, as shown in Figure 13.

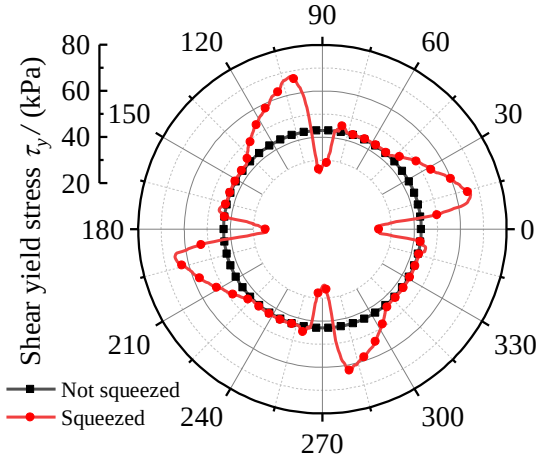

Figure 13. MRF shear yield stress distribution for squeezed and non-squeezed

The above figure shows the variation pattern of shear yield stress generated by MRF in two operating states of MRF, Figure 13 shows that the MRF shear yield stress in the polar coordinate system shows a periodic variation pattern in the working gap in the presence of a rectangular groove, when the center circle angle is 0° to 5°, the thickness of MRF working gap in the rectangular groove is thicker compared to the disc area, Therefore, the magnetic induction strength of MRF in the groove is small, resulting in the shear yield stress generated by MRF in the rectangular groove is smaller than the shear yield stress generated by MRF in the disc area, when the center circle angle is 5° to 14.5°, the MRF transitions from the rectangular slot region to the disc region, where the MRF is subject to squeeze stress. The shear stresses generated by MRF at this time are 42.2kPa and 67.7kPa, respectively.

This means that the MRF will produce an squeeze strengthening effect after being squeezed, and the MRF will produce a rapid increase in shear yield stress, so that the brake will produce a greater braking torque.

In conclusion, taking the same size planar disc drive as a comparison, the braking torque versus current curve of MRF brake after squeezing-strengthening can be derived from equation (4) with the results of magnetic and flow field analysis, as shown in Figure 14.

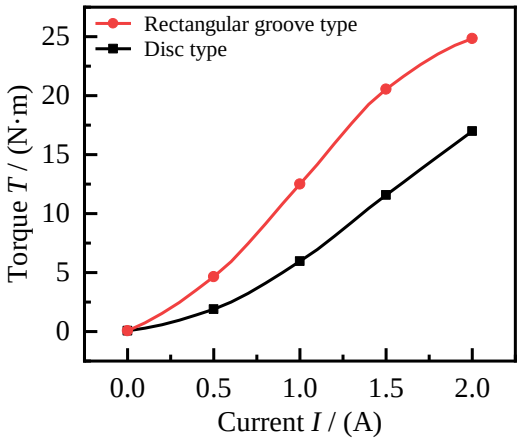

Figure 14. Relationship between current and torque of MRF brakes

As can be seen from Figure 14, the torque increases with the increase of current, and the rotor with rectangular grooves is able to produce a larger braking torque at the same current. The torque grows faster when the current is in the range of 0.5A to 1.5A. At a current of 2.0A, the brake torque reaches a maximum of 24.8N·m, which has a more excellent braking performance compared to the disc brake.

5. Conclusion

In this paper, the magnetic field and flow field analysis is carried out for a disc MRF brake with a wedge gap based on shear-squeeze mode. A simplified model of the magnetic field and flow field of the MRF brake is developed. The flow field simulation of the MRF brake is carried out by using the computational fluid dynamics method to derive the flow equations of MRF in the rotor. Based on the MRF squeeze strengthening theory, the braking torque versus the current curve of the brake was derived. The results of the study show that.

(1) MRF magnetic induction strength and initial yield stress increase with the increase of current. The magnetic induction strength in the rectangular groove is nonlinearly related to the circular center angle, and the MRF magnetic induction strength reaches a maximum value of 0.31 T in the rectangular groove region.

(2) The MRF linear velocity reaches a maximum value of 4.5 m/s at the rotor edge. the MRF is subjected to periodic squeezing stress through the wedge gap, and when the current is 2.0 A, the squeezing stress on the MRF reaches a maximum value of 80 kPa.

(3) The shear yield stress generated by MRF is consistent with the change of squeeze stress, and the shear yield stress reaches a maximum value of 67.7kPa at the transition area between the rectangular groove and the disc surface, and the torque generated by MRF brake after squeezing is 24.8N·m, which is 46.2% higher than the torque without squeezing.

Acknowledgments

The authors would like to gratefully acknowledge the National Natural Science Foundation of China (NO. 51875068, NO. 51905060), China Postdoctoral Science Foundation (2021M700619), and Science and Technology Research Program of Chongqing Municipal Education Commission under Grant KJQN201901107, Natural Science Foundation Project of Chongqing Science and Technology Commission (cstc2020jcyj-msxmX0346).

References

[1] Grunwald A, Olabi A G.Design of magneto-rheological (MR) valve[J].Sensors And Actuators a-Physical,2008, 148 (1): 211-223.

[2] Olabi A G, Grunwald A.Design and application of magneto-rheological fluid[J].Materials & Design,2007, 28 (10): 2658-2664.

[3] Tang X, Zhang X, Tao R, et al.Structure-enhanced yield stress of magnetorheological fluids[J].Journal of Applied Physics,2000, 87 (5): 2634-2638.

[4] Zhang Y, Li D, Zhang Z.The study of magnetorheological fluids sedimentation behaviors based on volume fraction of magnetic particles and the mass fraction of surfactants[J].Materials Research Express,2020, 6 (12).

[5] Park B J, Fang F F, Choi H J.Magnetorheology: materials and application[J].Soft Matter,2010, 6 (21): 5246-5253.

[6] Rabinow J.The magnetic fluid clutch[J].Electrical Engineering,1948, 67 (12): 1167-1167.

[7] Sun T, Peng X, Li J, et al.Testing device and experimental investigation to influencing factors of Magnetorheological fluid[J].International Journal of Applied Electromagnetics and Mechanics,2013, 43 (3): 283-292.

[8] Yang J, Chen S, Huang J, et al.Micro-analysis of slip differential heat of magnetorheological fluids based on micromechanics and microstructures[J].Materials Research Express,2019, 6 (6).

[9] Wu X, Huang C, Tian Z, et al.Development of a novel magnetorheological fluids transmission device for high-power applications[J].Smart Materials and Structures,2019, 28 (5).

[10] Mazlan S A, Issa A, Chowdhury H A, et al.Magnetic circuit design for the squeeze mode experiments on magnetorheological fluids[J].Materials & Design,2009, 30 (6): 1985-1993.

[11] Xiong Y, Huang J, Shu R Z.Research on Combined Transmission Performance of Magnetorheological Fluid and Electrothermal Shape Memory Alloys[J].China Mechanical Engineering,2021, 32 (17): 2040-2046.

[12] Becnel A C, Sherman S G, Hu W, et al.Squeeze strengthening of magnetorheological fluids using mixed mode operation[J].Journal of Applied Physics,2015, 117 (17).

[13] Hegger C, Maas J.Investigation of the squeeze strengthening effect in shear mode[J].Journal of Intelligent Material Systems and Structures,2016, 27 (14): 1895-1907.

[14] Bompos D A, Nikolakopoulos P G.CFD simulation of magnetorheological fluid journal bearings[J].Simulation Modelling Practice and Theory,2011, 19 (4).

[15] Susan-Resiga D, Bica D, Vékás L.Flow behaviour of extremely bidisperse magnetizable fluids[J].Journal of Magnetism and Magnetic Materials,2010, 322 (20).

[16] Chen W, Huang J, Yang Y.Research on the Transmission Performance of a High-Temperature Magnetorheological Fluid and Shape Memory Alloy Composite[J].Applied Sciences,2022, 12 (7).

[17] Yu M, Wang S, Fu J, et al.Unsteady analysis for oscillatory flow of magnetorheological fluid dampers based on Bingham plastic and Herschel–Bulkley models[J].Journal of Intelligent Material Systems and Structures,2013, 24 (9): 1067-1078.

[18] Xiong Y, Huang J, Shu R Z.Combined braking performance of shape memory alloy and magnetorheological fluid[J].Journal of Theoretical and Applied Mechanics,2021, 59 (3): 355-368.

[19] Sarkar C, Hirani H.Theoretical and experimental studies on a magnetorheological brake operating under compression plus shear mode[J].Smart Materials and Structures,2013, 22 (11).

[20] Danny B, Phil L, Bruce G.Miniature Single-Disk Viscous Pump (Single-DVP), Performance Characterization[J].Journal of Fluids Engineering,2006, 128 (3).

[21] Huang J, Chen X, Zhong L R.Analysis and Testing of MR Shear Transmission Driven by SMA Spring[J].Advances in Materials Science And Engineering,2013, 2013.

[22] Huang J, Zhang J Q, Yang Y, et al.Analysis and design of a cylindrical magneto-rheological fluid brake[J].Journal of Materials Processing Technology,2002, 129 (1-3): 559-562.

[23] Zhang X Z, Gong X L, Zhang P Q, et al.Study on the mechanism of the squeeze-strengthen effect in

magnetorheological fluids[J].Journal of Applied Physics,2004, 96 (4): 2359-2364.